Geometrical aspects of critical Ising configurations in two dimensions

Blöte, H.J.W.; Knops, Y.M.M.; Nienhuis, B.

Published in:
Physical Review Letters

DOI:
10.1103/PhysRevLett.68.3440

Geometrical Aspects of Critical Ising Configurations in Two Dimensions

H. W. J. Blöte,[1] Y. M. M. Knops,[1] and B. Nienhuis[2]
[1] *Laboratorium voor Technische Natuurkunde, Technische Universiteit Delft, P.O. Box 5046, 2600 GA Delft, The Netherlands*
[2] *Instituut voor Theoretische Fysica, Universiteit van Amsterdam, Valckenierstraat 65, 1018 XE Amsterdam, The Netherlands*
(Received 2 January 1992)

We present a physical interpretation of a number of exotic exponents of the two-dimensional Ising model, i.e., exponents that do have a conformal classification, but outside the unitary grid. They describe the scaling behavior of geometric properties of Ising and random clusters. For instance, the probability that two spins at a distance r lie on the perimeter of the same Ising cluster decays as $r^{-5/4}$ at criticality. These results are obtained via mappings on the Coulomb gas. A part of the Coulomb gas scenario is verified by means of finite-size scaling of transfer-matrix results.

PACS numbers: 64.60.Ak, 05.50.+q, 64.60.Cn, 75.10.Hk

The solution of the two-dimensional Ising model has yielded exact results for a number of observable quantities such as the energy, the spontaneous magnetization, and the spin-spin correlation function. More generally, it describes properties that can be directly expressed in expectation values of products of spin variables. They correspond with singularities in the free energy as a function of the temperature and the magnetic field. The associated exponents fit the Kac formula as predicted by the theory of conformal invariance [1, 2], i.e., scalar observables have scaling dimensions

$$X_{i,j} = \frac{(4i-3j)^2-1}{24} \quad \text{with} \quad 1 \le i \le 2, \quad 1 \le j \le 3 . \tag{1}$$

We shall refer to these permitted values (i,j) as "unitary grid."

A class of quantities falls outside this category: These concern geometrical aspects of Ising and random-cluster configurations, e.g., percolation, that cannot simply be formulated as products of spin variables. The associated "exotic" exponents do not contribute to the thermodynamic singularity at the Ising critical point. Indeed, conformal invariance shows that the algebra associated with the unitary grid is closed, and thus decoupled from the exotic operators.

An example is the irrelevant Ising dimension $X_{\rm ir} = \frac{10}{3}$ [3]. The conformal classification of this exponent as $X_{3,1}$ is *outside* the unitary grid. Barma and Fisher [4] report some evidence for its presence in continuous-spin models, but it does not show up in exact solutions, nor in finite-size results for Ising-like models [5]. As predicted by one of us [3], it is, however, present in derivatives of the correlation length of the $q = 2$ states random-cluster model with respect to q [5]. This differentiation yields expectation values containing the number of random-cluster loops and components, in analogy with the description of the percolation problem by means of the $q = 1$ Potts model. Another example is the dimension $X_h = \frac{5}{96}$ [3, 6] governing the probability that two distant spins are members of the same Ising cluster. An Ising cluster is defined as a group of spins connected by bonds placed between all pairs of parallel neighbors.

These examples provide a clue to the physical meaning of the exotic exponents. In this Letter we therefore determine the critical exponents of a number of percolation-related correlation functions in the Ising model by means of the Coulomb gas technique. Indeed, we find that these exponents match Eq. (1) with (i,j) *outside* the unitary grid. Before proceeding with the actual derivations, we summarize our main results.

Let $g_{ip}(r)$ describe the probability that two points at a distance r lie at the perimeter of the same Ising cluster. The large-r critical behavior of this correlation function is

$$g_{ip}(r) \sim r^{-2X_{ip}} \quad \text{with} \quad X_{ip} = \tfrac{5}{8} = X_{2,4} . \tag{2}$$

By $g_{rp}(r)$ we denote the probability that two points at a distance r lie at the perimeter of the same $q = 2$ random cluster. A random cluster is a group of spins connected by the bonds of the random-cluster model. These bonds occur between parallel neighbor spins with a probability $p = 1 - e^{-K}$, where K is the Ising coupling (see below). At criticality this correlation function satisfies

$$g_{rp}(r) \sim r^{-2X_{rp}} \quad \text{with} \quad X_{rp} = \tfrac{1}{3} = X_{3,3} . \tag{3}$$

Furthermore, let $g_{ii}(r)$ describe the probability that two Ising clusters touch at two points separated by a distance r. This correlation function obeys

$$g_{ii}(r) \sim r^{-2X_{ii}} \quad \text{with} \quad X_{ii} = \tfrac{21}{8} = X_{1,4} . \tag{4}$$

Finally, by $g_{rr}(r)$ we denote the probability that two $q = 2$ random clusters touch at two points separated by a distance r. This correlation function behaves as

$$g_{rr}(r) \sim r^{-2X_{rr}} \quad \text{with} \quad X_{rr} = \tfrac{35}{24} = X_{3,2} . \tag{5}$$

It will also be shown below that the dimensions X_{rr} and X_{ii} govern the crossover from random clusters to Ising

clusters.

Percolation aspects of the Ising model can be described by means of a dilute $q = 1$ state Potts model. The site dilution of this model is accounted for by interacting Ising lattice gas variables $t_k = 0$ or 1. After introducing the $q = 1$ random-cluster expansion, i.e., bond variables $b_{ij} = 0$ or 1 [7], and keeping track of powers of q for future purposes, the Ising partition function becomes

$$Z_{\mathrm{RC}} = \sum_{\{t,b\}} q^{n_c} \prod_{\langle ij \rangle} w_{ij} , \tag{6}$$

where n_c is the number of percolation clusters (q=1 random clusters) and w_{ij} is the weight factor per nearest-neighbor pair i and j:

$$w_{ij} = (1 - b_{ij})\{(1 - t_i)(1 - t_j) + (t_i + t_j - 2t_i t_j)e^{-K}\} + \{b_{ij}p + (1 - b_{ij})(1 - p)\}t_i t_j , \tag{7}$$

where K is the Ising lattice gas coupling, $p = 1 - e^{-L}$, and L is the $q = 1$ Potts coupling. The bond variables in Eq. (6) enable the calculation of certain percolation-related correlation functions. This is no longer possible after summation over $\{b\}$ in Eq. (6), which trivially reproduces the Ising partition function. The parameter p governs the bond percolation between neighboring occupied ($t_i = t_j = 1$) sites; it does not influence the Ising-like singularity at the line $K = K_c$ labeled CI in Fig. 1.

It is noteworthy that the $q = 2$ random-cluster model generates similar graphs as Eq. (6). After introducing bond variables $b_{ij} = 0$ or 1 as in the $q = 2$ random-cluster expansion, but *without* summation over the Ising degrees of freedom, the bond weights assume the same form as in Eq. (7). The difference, namely that in the $q = 2$ random-cluster model clusters of $-$ spins may exist besides those of $+$ spins, is irrelevant as far as percolation within clusters is concerned. The $q = 2$ random-cluster model imposes a probability $p = 1 - e^{-K}$ on bonds between parallel spins; this is shown by line RC in Fig. 1.

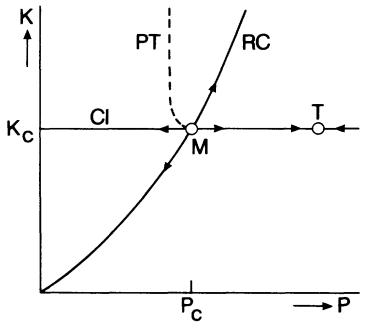

FIG. 1. Phase diagram of the model described by Eq. (6). The line CI is an Ising critical line; the line RC represents the $q = 2$ random-cluster model. The multicritical point M acts as the percolation threshold on line CI. The broken line PT sketches the percolation transition in the ordered Ising model.

Under renormalization, the lines CI and RC in Fig. 1 should be flow lines. Thus, the intersection M plays the role of a multicritical fixed point. The exponent governing the flow along RC away from M is the Ising temperature dimension $X_t = 1$. The exponent describing instead the bond dilution flow along CI was determined as $X_{rr} = 1.465$ by Coniglio and Klein [8] using the Migdal-Kadanoff approximation. In this renormalization picture, X_{rr} describes the crossover from the Ising fixed point M to the tricritical $q = 1$ Potts range $p > p_c = 1 - e^{-K_c}$. This range is governed by an attractive fixed point T [9] with an irrelevant exponent X_{ii}.

In order to derive X_{rr} and X_{ii} we consider the correlation between two bond dilution operators p_0 and p_r acting in points separated by a distance r. Since the free energy $f = \ln Z_{\mathrm{RC}}$ is independent of p, we use instead the number of percolation clusters $\langle n_c \rangle = \partial \ln Z_{\mathrm{RC}}/\partial q$ as a generating function for the desired correlations. The interaction $\partial^2\langle n_c \rangle/\partial p_0\, \partial p_r$ between the bond dilution operators is accounted for by those percolation graphs in which bonds 0 and r close a common loop, i.e., removal of both bonds decomposes one percolation cluster in two disjoint clusters. After the well-known mapping [10] of the random-cluster model (point M in Fig. 1) on the six-vertex model, these graphs are precisely those generated by placing a vertex with four outgoing arrows on bond 0 and one with four incoming arrows on bond r [Fig. 2(a)]. These two vertices must be connected to one another via paths of arrows; thus there are two random clusters spanning the distance between 0 and r, sandwiched between dual clusters (vacuum). This diagram was used by den Nijs [11] to study the cubic crossover of the Potts model;

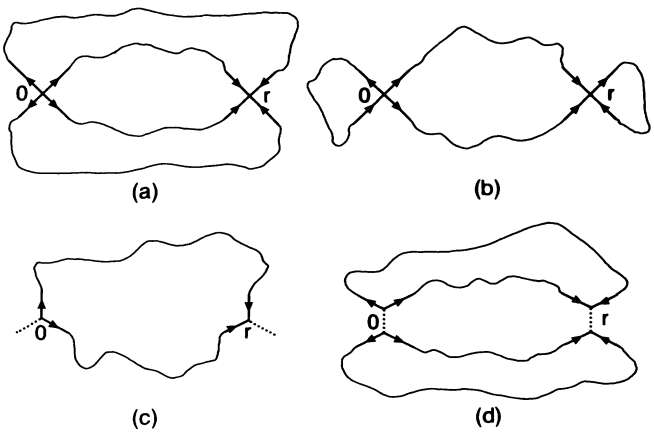

FIG. 2. Vertex diagrams associated with correlation functions involving different sorts of clusters: random clusters (sites percolating via bond variables) or Ising clusters (spins of one sign connected via nearest-neighbor paths). The square lattice is used for the description of (a),(b) random clusters and the honeycomb lattice is used for (c),(d) Ising clusters. Points 0 and r may be connected via two clusters [(a) and (d)] or one [(b) and (c)].

thus, it is well known how to proceed with the subsequent mapping on the Coulomb gas [12, 13]. The newly added vertices map on magnetic charges $m_0 = -m_r = 2$; the renormalized coupling constant is $g_R = \frac{3}{4}$. A problem associated with ambiguous solid-on-solid (SOS) heights is solved by adding electric charges $e_0 = e_r = \frac{1}{4}$, which neutralize the ambiguous phase factors [13]. The associated scaling dimension is

$$X(e,m) = -\frac{e_0 e_r}{2g_R} - \frac{m_0 m_r g_R}{2} \tag{8}$$

so that $X_{rr} = \frac{35}{24}$.

Another correlation function involving the geometry of the random-cluster model is associated with vertices with three outgoing and one incoming arrow or vice versa, i.e., with magnetic charges ± 1 in the Coulomb gas. A typical way to connect these vertices is shown in Fig. 2(b): Sites 0 and r are restricted to the perimeter of the same random cluster. The same electric charges as before are added to neutralize unwanted phase factors. Thus, Eq. (8) yields $X_{rp} = \frac{1}{3}$.

We proceed with the case $p = 1$, assumedly within the domain of attraction of the fixed point T in Fig. 1. Thus the percolation clusters coincide with the Ising clusters. By interpreting the loops surrounding these clusters as steps in an SOS surface one obtains another mapping of the Ising model on the Coulomb gas; equivalently, one may take $n = 1$ in the procedure for the O(n) model [14]. Here we may conveniently choose the triangular lattice so that the loops, which lie on the honeycomb lattice, do not intersect. The honeycomb vertices describing the corresponding SOS model have one incoming and one outgoing arrow, or no arrows at all. Instead of the vertices of Fig. 2(b), we now use honeycomb vertices with two incoming arrows or two outgoing arrows [Fig. 2(c)]. We use neighbor pairs of such vertices [14] [Fig. 2(d)] to replace those in Fig. 2(a). The lines connecting the vertices now separate regions of + and − spins instead of different random clusters.

The diagram shown in Fig. 2(c) is obviously associated with the probability that two spins lie at the perimeter of the same Ising cluster of, e.g., + spins. The magnetic charges are $m = \pm 1$. Again we use electric charges to neutralize the ambiguity of the SOS heights at points 0 and r. Since the loop weights are now different, so are the charges: $e_0 = e_r = \frac{1}{3}$, while $g_R = \frac{4}{3}$ [13]. According to Eq. (8), the dimension X_{ip} governing the decay of this correlation function is $X_{ip} = \frac{5}{8}$.

The correlation function associated with Fig. 2(d) concerns the probability that two otherwise disconnected clusters of, e.g., + spins touch at positions 0 and r. The mapping of this diagram on the Coulomb gas, which was described by one of us [13] for a determination of the cubic crossover exponent of the O(n) model, leads to magnetic charges ± 2 and electric charges $\frac{1}{3}$. Thus, from Eq. (8), we obtain the irrelevant dimension $X_{ii} = \frac{21}{8}$. It describes (in analogy with X_{rr}) the renormalization flow along line CI to T in Fig. 1.

While many striking successes have been obtained by Coulomb gas methods, one has to rely on assumptions [13] so that it is appropriate to check the results numerically. Monte Carlo results [15] for the triangular Ising model confirm that $X_{ip} = \frac{5}{8}$ within 1%. Accurate results may also be obtained by finite-size scaling of transfer-matrix results [16]. The transfer matrix for the random-cluster model [17] can easily be generalized to include vacancies. Thus we devised an algorithm to enumerate the generalized magnetic connectivities (i.e., the degrees of freedom associated with a free surface) implied by Eq. (6). A partial ordering of the connectivities follows from the number and the position of the vacancies; the remaining problem (an ordering of connectivities without vacancies) is solved in Ref. [17]. Evaluation of the two largest eigenvalues of this asymmetric transfer matrix, for which efficient methods are available [17], yields the magnetic correlation length ξ_h associated with the probability that two sites are members of the same random cluster. Such data were obtained for cylindrical systems spanning up to $L = 11$ lattice units; the latter size has a transfer matrix of dimension 5 593 438. The theory of conformal invariance [2, 18] relates the finite-size scaling behavior of ξ_h, and thereby the two largest eigenvalues Λ_0 and Λ_1, to the magnetic dimension X_h. Thus

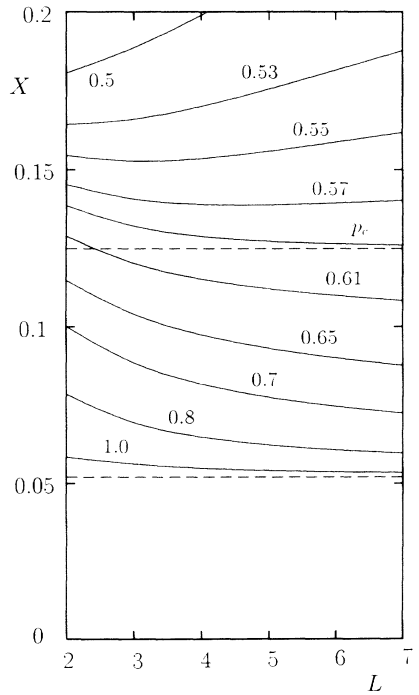

FIG. 3. Finite-size data $X(p, L)$, connected by smooth lines. These data agree well with the predicted renormalization flow [8] and with the expected dimensions $X_m = \frac{1}{8}$ at $p = p_c$ and $X_h = \frac{5}{96}$ for $p > p_c$ (broken lines).

TABLE I. Finite-size estimates $X_h(p=1,L)$ of the $q=1$ tricritical magnetic Potts scaling dimension X_h, and $X_{rr}^{(k)}(L)$ $(k=1,2)$ of the dimension X_{rr} associated with bond dilution of the $q=2$ random-cluster model.

L	$X_h(1,L)$	$X_{rr}^{(1)}(L)$	$X_{rr}^{(2)}(L)$
2	0.058 44	1.4433	1.4168
3	0.056 29	1.4508	1.4318
4	0.054 89	1.4502	1.4409
5	0.054 15	1.4500	1.4459
6	0.053 73	1.4504	1.4488
7	0.053 47	1.4511	1.4507
8	0.053 29	1.4518	1.4519
9	0.053 15	1.4524	1.4529
10	0.053 05		
11	0.052 97		

$$X(p,L) = (L/2\pi)\ln\Lambda_0/\Lambda_1 \tag{9}$$

are finite-size estimates of X_h. This quantity was computed for several values of p and L at $K=K_c$ (see Fig. 3). For $p=p_c$ the data converge, as expected, to the Ising value $X_m=\frac{1}{8}$. The L dependence of the other data confirm the renormalization flow as found by Coniglio and Klein [8]. With increasing L, the data points move away from $X_m=\frac{1}{8}$; thus the fixed point M is unstable. The flow for $p<p_c$ is towards the vacuum $p=0$, and for $p>p_c$ towards a high-p fixed point T: the $q=1$ Potts tricritical point. The finite-size data show that intermediate fixed points are absent, and that the corrections to scaling become small near $p=1.1$. Values of $X(p=1,L)$ are given in Table I. Extrapolation (see, e.g., Ref. [17]) yields $X_h=0.052\,06(5)$, in perfect agreement with the Coulomb gas result $\frac{5}{96}$ [3, 6].

Also X_{rr} can be found numerically by computing the derivative of Eq. (9) with respect to p at p_c. Finite-size scaling predicts that

$$\left[\frac{d^kX(p,L)}{dp^k}\right]_{p=p_c} \sim L^{k(2-X_{rr})} \tag{10}$$

so that X_{rr} can be estimated (for details see Ref. [17]) from the numerical data. These estimates are included in Table I for $k=1$ and 2. Extrapolation [17] yields $X_{rr}=1.455(5)$ for $k=1$ and 1.460(1) for $k=2$, in good agreement with the value $\frac{35}{24}$ derived above.

This work is part of the research program of the "Stichting voor Fundamenteel onderzoek der Materie" (FOM) which is financially supported by the Nederlandse Organisatie voor Wetenschappelijk Onderzoek" (NWO).

[1] A. A. Belavin, A. M. Polyakov, and A. B. Zamolodchikov, J. Stat. Phys. **34**, 763 (1984); Nucl. Phys. **B241**, 333 (1984); D. Friedan, Z. Qiu, and S. Shenker, Phys. Rev. Lett. **52**, 1575 (1984).
[2] J. L. Cardy, in *Phase Transitions and Critical Phenomena*, edited by C. Domb and J. L. Lebowitz (Academic, London, 1987), Vol. 11.
[3] B. Nienhuis, J. Phys. A **15**, 199 (1982).
[4] M. Barma and M. E. Fisher, Phys. Rev. Lett. **53**, 1935 (1984); Phys. Rev. B **31**, 5954 (1985).
[5] H. W. J. Blöte and M. P. M. den Nijs, Phys. Rev. B **37**, 1766 (1988).
[6] B. Duplantier and H. Saleur, Phys. Rev. Lett. **63**, 2536 (1989).
[7] P. W. Kasteleyn and C. M. Fortuin, J. Phys. Soc. Jpn. Suppl. **46**, 11 (1969).
[8] A. Coniglio and W. Klein, J. Phys. A **13**, 2775 (1980).
[9] B. Nienhuis, A. N. Berker, E. K. Riedel, and M. Schick, Phys. Rev. Lett. **43**, 737 (1979).
[10] H. N. V. Temperley and E. H. Lieb, Proc. R. Soc. London A **322**, 251 (1971); R. J. Baxter, S. B. Kelland, and F. Y. Wu, J. Phys. A **9**, 397 (1976).
[11] M. P. M. den Nijs, J. Phys. A **17**, L295 (1984).
[12] L. P. Kadanoff, J. Phys. A **11**, 1399 (1978).
[13] B. Nienhuis, in *Phase Transitions and Critical Phenomena* (Ref. [2]).
[14] B. Nienhuis, Phys. Rev. Lett. **49**, 1062 (1982).
[15] H. W. J. Blöte (unpublished).
[16] For reviews, see M. P. Nightingale, J. Appl. Phys. **53**, 7927 (1982); and M. N. Barber, in *Phase Transitions and Critical Phenomena*, edited by C. Domb and J. L. Lebowitz (Academic, London, 1983), Vol. 8.
[17] H. W. J. Blöte and M. P. Nightingale, Physica (Amsterdam) **112A**, 405 (1982).
[18] J. L. Cardy, J. Phys. A **17**, L385 (1984).